Sphingomyelin Acyl Chains Influence the Formation of Sphingomyelin- and Cholesterol-Enriched Domains

Oskar Engberg,[1] Kai-Lan Lin,[1] Victor Hautala,[1] J. Peter Slotte,[1] and Thomas K. M. Nyholm[1,*]
[1]Biochemistry, Faculty of Science and Engineering, Abo Akademi University, Turku, Finland

ABSTRACT   The segregation of lipids into lateral membrane domains has been extensively studied. It is well established that the structural differences between phospholipids play an important role in lateral membrane organization. When a high enough cholesterol concentration is present in the bilayer, liquid-ordered (L_o) domains, which are enriched in cholesterol and saturated phospholipids such as sphingomyelin (SM), may form. We have recently shown that such a formation of domains can be facilitated by the affinity differences of cholesterol for the saturated and unsaturated phospholipids present in the bilayer. In mammalian membranes, the saturated phospholipids are usually SMs with different acyl chains, the abundance of which vary with cell type. In this study, we investigated how the acyl chain structure of SMs affects the formation of SM- and cholesterol-enriched domains. From the analysis of *trans*-parinaric acid fluorescence emission lifetimes, we could determine that cholesterol facilitated lateral segregation most with the SMs that had 16 carbon-long acyl chains. Using differential scanning calorimetry and Förster resonance energy transfer techniques, we observed that the SM- and cholesterol-enriched domains with 16 carbon-long SMs were most thermally stabilized by cholesterol. The Förster resonance energy transfer technique also suggested that the same SMs also form the largest L_o domains. In agreement with our previously published data, the extent of influence that cholesterol had on the propensity of lateral segregation and the properties of L_o domains correlated with the relative affinity of cholesterol for the phospholipids present in the bilayers. Therefore, the specific SM species present in the membranes, together with unsaturated phospholipids and cholesterol, can be used by the cell to fine-tune the lateral structure of the membranes.

SIGNIFICANCE   The membranes in mammalian cells contain a complex mixture of lipids and proteins. A reason for containing a large number of different lipids with deviating structures is that it allows the membrane to structurally rearrange into lateral and transbilayer domains with different properties. Likely, these kinds of structural domains within the cellular membranes are contributing to the regulation of different processes in cells, e.g., by regulating the activity and distribution of membrane proteins. The data presented here together with previously published recent studies are contributing to our understanding of the forces that drive the self-organization of lipids and will help us to predict how different lipids affect the structure-function of cellular membranes.

INTRODUCTION

Mammalian membranes are composed of a vast number of diverse lipids, mainly phospholipids and cholesterol (1). It is well documented that these kinds of lipids in model membranes can segregate into lateral domains because of structural differences between lipid components (1,2). It is still not known to what degree this kind of lateral segregation occurs in the membranes of living cells. In addition, the forces driving the lateral segregation of lipids into domains are not yet fully understood. A convenient approach to examine both the probability of lateral segregation in cellular membranes and the mechanisms driving the formation of such segregation involves the use of simple three-component model membranes that roughly mimic the membranes of mammalian cells (2,3).

Cholesterol is an essential lipid in mammalian membranes, and because of its molecular structure, it modulates the physiochemical properties of the surrounding lipid bilayer. For example, cholesterol has a great impact on the acyl chain order of neighboring phospholipids, and when abundant in a high enough concentration, it forms a

liquid-ordered (L_o) phase together with the surrounding saturated phospholipids (4,5). Cholesterol is known to preferentially interact with phospholipids that have saturated acyl chains, and the more double bonds the acyl chains of a phospholipid have, the lower the affinity of the sterol for lipids becomes (6–8). Similarly, the lengths of the acyl chains and the headgroups of phospholipids seem to be the determinants of how strongly they interact with cholesterol (8–15).

In a ternary lipid bilayer composed of an unsaturated phospholipid, a saturated phospholipid, and cholesterol, the lipid components may segregate laterally into L_o and fluid-disordered (L_d) domains with different lipid compositions (16). How prone this system is to forming lateral domains of course depends foremost on the lipid composition. Recently, we observed a correlation between the relative affinity of cholesterol for the two phospholipids in the bilayer and the probability of lateral segregation (6,9). In other words, the larger the preference of cholesterol for the saturated phospholipid over the unsaturated lipid, the more cholesterol facilitates a lateral segregation of the two phospholipids. This can also be thought of as a push-pull mechanism in which the unsaturated phospholipids repel cholesterol, whereas the saturated phospholipids attract the sterol, as discussed by Regen and co-workers (17,18). Hence, the structure of both the unsaturated and saturated lipids present in the bilayer can be expected to determine the extent to which cholesterol can promote lateral segregation.

It has previously been observed that when 1,2-dipalmitoyl-*sn*-glycero-3-phosphocholine (DPPC) was chosen as the saturated phospholipid instead of *N*-palmitoyl sphingomyelin (PSM), the impact of cholesterol on lateral structuring of the membrane was markedly smaller (6). This effect can be explained by the significantly lower affinity of cholesterol for DPPC compared to PSM. However, the promoting effect of cholesterol on lateral segregation has been tested only with these two saturated phospholipids. Therefore, this study aimed to broaden our understanding of the role of saturated lipids in the processes governing the formation of cholesterol-enriched domains. For this, sphingomyelins (SMs) with different acyl chains were compared in ternary and binary lipid compositions. This comparison gave information of how the interactions of SM acyl chains with cholesterol and unsaturated lipids influence lateral segregation and offered insights into how different SMs may function in cellular membranes. This is important, especially because it is known that SM acyl chain composition varies widely between cell types and mammalian species (19,20). By mixing SMs with different acyl chain lengths with phosphatidylcholines (PCs) with defined acyl chains, information was also obtained regarding the role of hydrophobic matching between lipids in the formation of cholesterol-enriched lateral domains.

We determined the effect of cholesterol on lateral segregation by comparing binary phospholipid bilayers with 0 and 20 mol % cholesterol. The formation of lateral domains was determined from time-resolved fluorescence measurements with *trans*-parinaric acid (tPA). The thermotropic behavior of different lipid systems was investigated using differential scanning calorimetry (DSC) and Förster resonance energy transfer (FRET) techniques. From these results, we could draw conclusions about the structural determinants for lateral segregation and properties of lateral domains and evaluate how these properties related to the determined affinities of cholesterol for the different phospholipids that were present in the bilayers. The role of cholesterol as a modulator of lateral membrane structure has been discussed.

MATERIALS AND METHODS

Material

The phospholipids 1-palmitoyl-2-oleoyl-*sn*-glycero-3-phosphocholine (POPC), 1,2-oleoyl-*sn*-glycero-3-phosphocholine (DOPC), 1-palmitoyl-2-arachidonoyl-*sn*-glycero-3-phosphocholine (PAPC), rhodamine-1,2-dioleoyl-*sn*-3-glycero-3-phosphoethanolamine (Rho-DOPE), *N*-stearoyl-D-erythro-SM (18:0-SM), *N*-lignoceroyl-D-erythro-SM (24:0-SM), *N*-nervonoyl-D-erythro-SM (24:1-SM), sphingosylphosphorylcholine, and egg SM were obtained from Avanti Polar Lipids (Alabaster, AL). *N*-palmitoyl-D-erythro-SM (16:0-SM) was purified from egg SM by reversed-phase high-performance liquid chromatography (Discovery C18; Sigma-Aldrich Supelco (St. Louis, MO); dimensions 250.0 × 21.2 mm, 5 μm particle size), using methanol as an eluent. *N*-myristoyl-D-erythro-SM (14:0-SM) was synthesized as previously described (21). The purity and identity of 14:0-SM and 16:0-SM were verified by electrospray ionization mass spectrometry. Cholesterol and methyl β-cyclodextrin were purchased from Sigma-Aldrich (St. Louis, MO). Cholesta-5,7,9-triene-3-β-ol (CTL) (11) was prepared according to published procedures (22,23). tPA was synthesized as described in (24) and purified from hexane by crystallization (25). It was stored at $-80°C$ and contained 1 mol % butylated hydroxytoluene to prevent oxidation. Stock solutions of diphenylhexatriene (DPH; Molecular Probes, Eugene, OR), tPA, Rho-DOPE, and CTL were prepared in ethanol. Fluorophore concentrations were determined on the basis of their respective molar extinction coefficients: CTL (11,250 cm^{-1} M^{-1}), DPH (92,000 cm^{-1} M^{-1}), Rho-DOPE (90,000 cm^{-1} M^{-1}), and tPA (88,000 cm^{-1} M^{-1}). The concentrations of all phospholipid stock solutions were determined according to (26). Cholesterol concentration was determined using a surface barostat (27). All solutions were stored in the dark at $-20°C$ and warmed to ambient temperature before use. The water used in all the experiments was purified by reverse osmosis, followed by a passage through a Milli-Q UF-Plus water purification system (MilliporeSigma, Billerica, MA) to yield a product resistivity of 18.2 mΩ cm.

Time-resolved emission spectroscopy

All fluorescence experiments were performed with multilamellar vesicles (MLVs). In brief, the MLVs were made as follows. Lipids and fluorophores were mixed in methanol, after which the solvent was evaporated to create a lipid film in the glass tube. The lipids in the film were hydrated 30 min in Milli-Q water at 65°C, after which the tubes were vortexed to create MLVs. After this, the samples were bath sonicated at 65°C for 5 min.

The formation of ordered SM-enriched (gel or L_o) domains was detected from the average lifetime of tPA emission. The excited-state lifetime of tPA

is very sensitive to the order of its local environment (25,28,29); hence, its emission lifetime varies in fluid and highly ordered membrane domains (30,31). The fluorescence lifetimes of tPA (1 mol %) were measured in MLVs, with a final lipid concentration of 0.1 mM. A FluoTime 100 spectro-fluorometer with a TimeHarp 260 Pico time-correlated single photon-counting module (PicoQuant, Berlin, Germany) was used for measurements. tPA was excited with a 297 $\pm$ 10 nm light-emitting diode laser source (PLS 300; PicoQuant), and the emission was collected through a 435/40 nm single-bandpass filter. Fluorescence decays were recorded at the denoted temperatures (temperature controlled by water bath), with constant stirring during measurements. Data were analyzed using FluoFit Pro software obtained from PicoQuant. The decay was described by the sum of exponentials, where α_i was the normalized pre-exponential, and τ_i was the lifetime of decay of component i. The intensity-weighted average lifetime is given as follows:

$$\langle \tau \rangle = \frac{\sum_i \alpha_i \tau_i^2}{\sum_i \alpha_i \tau_i}. \tag{1}$$

FRET

The FRET technique was used to detect the thermostability of L_o domains. For these experiments, the F_0 samples had the lipid composition of unsaturated PC/SM/cholesterol (40:40:20) and contained 0.5 mol % DPH. The F samples had the same lipid composition but contained both 0.5 mol % DPH and 2.0 mol % Rho-DOPE. The total lipid concentration in both the F and F_0 samples was 100 μM. The MLVs used in these measurements were prepared as described above. The emission spectra were recorded on a Quanta-Master spectrofluorometer (Photon Technology, Lawrenceville, NJ) at defined temperatures. The excitation wavelength was set to 358 nm, and the emission was measured from 380 to 650 nm. The FRET efficiency was determined from the fluorescence intensity at 430 nm in the F and F_0 samples.

DSC

MLVs composed of the indicated lipids were prepared by the hydration of dried lipid films in glass tubes. The lipids were hydrated for 30 min at 65°C in Milli-Q water before being briefly vortexed and loaded into the sample cell of a MicroCal VP-DSC instrument (MicroCal, Northampton, MA). The final lipid concentration was 1.5 mM in all samples. The temperature ramp rate was 1°C min^{-1}. The data were analyzed using Origin software (MicroCal).

RESULTS

Formation of lateral SM-enriched domains

The formation of lateral membrane domains enriched in SM and cholesterol was determined on the basis of time-resolved fluorescence measurements of tPA in bilayers, with systematically varied phospholipid compositions. As the emission lifetime of tPA is strongly dependent on the phase state and acyl chain order in the bilayer, it is a sensitive reporter of changes related to these parameters in the bilayer (30). Fig. 1 shows representative data from bilayers composed of POPC and SM (16:0-SM, 18:0-SM, or 24:0-SM), with or without 20 mol % cholesterol. With 14:0-SM and 24:1-SM, no lateral segregation was observed at 23°C. Whereas the cholesterol content was kept constant
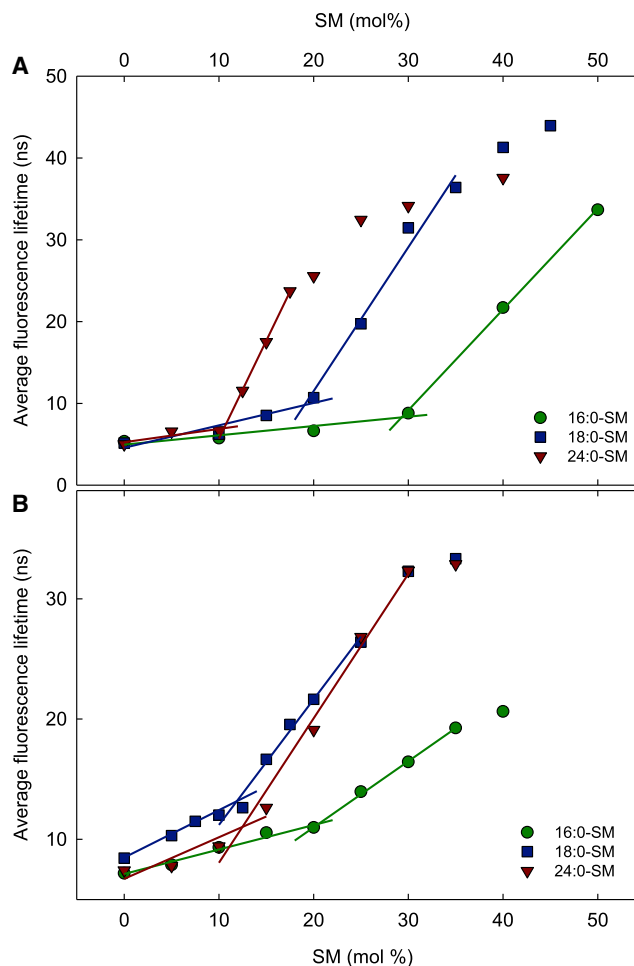

FIGURE 1 The determination of ordered domain formation on the basis of tPA fluorescence lifetime. Representative data from experiments with 16:0-SM, 18:0-SM, and 24:0-SM in POPC performed at 23°C are shown. Experiments were conducted with 0 mol % (A) and 20 mol % (B) cholesterol in the bilayers. To determine the SM amount needed to form ordered domains, the data were fitted with straight lines, one to the slowly rising slope at the low SM content and one to the initial linear part of the steeply rising part. The crossing point of the two lines was defined as the SM concentration at which ordered domains started to form. To see this figure in color, go online.

(0 or 20 mol %), the SM concentration was increased from 0 to 50 mol %. Initially, the emission lifetime of tPA increased slightly as the SM content was raised, but when the SM concentration reached a critical level, the lifetimes increased much more dramatically.

This dramatic change in the average lifetime, which is usually accompanied by the appearance of a new long life-time component (9), indicated the presence of ordered (gel or L_o) domains in the bilayers and the solubility limit of the particular SM in the L_d phase bilayer. The solubility limit of SM was quantified by fitting two linear functions to the obtained data: one to the initial moderate slope and one to the linear initial part of the steep slope (see Fig. 1). The solubility limit of SM in the L_d phase bilayer was

defined as the intercept of two linear functions. The quantified solubility limits of SM from all studied systems are shown in Fig. 2.

From the data, it was clear that the longer the SM acyl chains, the lower the solubility of SM in the cholesterol-free L_d phase PC bilayer (Figs. 1 A and 2, A and B). This was the case in both POPC and PAPC bilayers, and it showed that the formation of the gel phase in all the studied PC-SM systems depended on the length of SM acyl chains. The inclusion of 20 mol % cholesterol decreased the impact of the length of SM acyl chains on lateral segregation, especially in PAPC bilayers (Fig. 2 B), where all tested SM molecules had a similar solubility limit in the presence of 20 mol % cholesterol.

The role of cholesterol as a facilitator of lateral segregation was evaluated by comparing the solubility limit of SM in fluid PC bilayers, with or without cholesterol. From Fig. 2 A, it is clear that in POPC bilayers, cholesterol facilitated the formation of ordered domains most together with 16:0-SM and 18:0-SM, whereas in bilayers with 24:0-SM, cholesterol did not alter the solubility limit of SM. With the polyunsat-

urated PAPC, the effect of cholesterol on the formation of lateral domains decreased with the length of the SM acyl chains, but in these bilayers, cholesterol facilitated segregation also in the presence of 24:0-SM. These differences between the POPC and PAPC bilayers are in agreement with previous observations regarding how the number of double bonds in PC acyl chains can increase the promoting effect of cholesterol on lateral segregation (6).

Temperature dependence of lateral segregation

To address how temperature affected the lateral segregation of different SM molecules into SM-enriched domains, we measured the solubility of 16:0-SM and 24:0-SM in fluid POPC bilayers at different temperatures. These two SMs were chosen as they represented the most different of the three SMs that showed domain formation at 23°C (see Fig. 2). The experimental setup was the same as that discussed above. Again, the effect of cholesterol was assessed by a comparison of bilayers with 0 and 20 mol % cholesterol.

Fig. 3 A shows how the solubility of 16:0-SM in fluid POPC was affected by temperature. Without cholesterol, the solubility was markedly affected by increased temperature, which is in good agreement with previous observations (32). At 23°C, lateral segregation occurred when ∼30 mol % 16:0-SM was present in the bilayer. When the temperature reached 37°C, around 70 mol % 16:0-SM was solubilized in POPC before a gel phase formed. At 42°C, no gel phase was detected. With 20 mol % cholesterol, the solubility of 16:0-SM in POPC was not as sensitive to temperature (Fig. 3 A). Up to a temperature greater than 30°C, ∼20 mol % SM was solubilized in the fluid POPC bilayer before lateral segregation into SM-enriched domains occurred. However, at 37°C, the solubility limit was clearly higher. A comparison of the results with and without cholesterol indicated that the sterol facilitated the formation of lateral 16:0-SM-enriched domains more as the temperature was increased toward physiological temperature.

With 24:0-SM in POPC, the temperature effect was different (Fig. 3 B). An increased temperature affected the solubility of 24:0-SM in fluid POPC less than that observed with 16:0-SM. Without cholesterol, the SM-enriched gel phase started to form above 33 mol % 24:0-SM even at 42°C. In bilayers with 24:0-SM, cholesterol had no significant promoting effect on the formation of lateral SM-enriched domains at any temperature, which is in contrast to what was observed with 16:0-SM.

Thermostability of SM-enriched domains in binary phospholipid bilayers

To gain insights into the interactions between PC and SM molecules, we performed DSC measurements with MLVs of POPC or PAPC mixed in a molar ratio of 1:1 with a broad
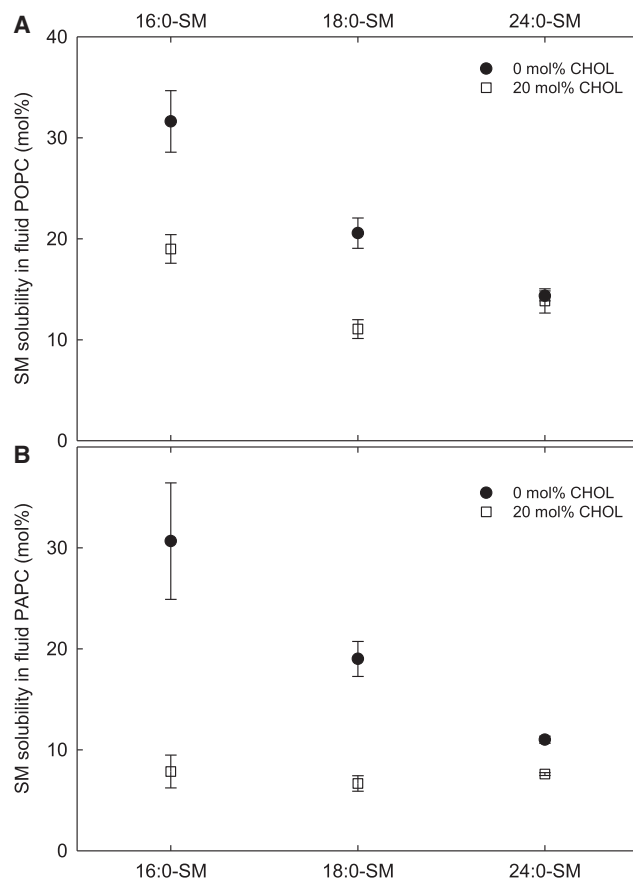

FIGURE 2 The effect of cholesterol on the solubility limits of different SMs in the L_d phase. The solubility of the SMs in the L_d phase was measured at 23°C in POPC (A) and PAPC (B) bilayers containing 0 or 20 mol % cholesterol. Above these concentrations, the SMs formed ordered domains. The values are averages of ≥3 experiments ± SD.

FIGURE 3 The effect of temperature on the solubility limits of different SMs in the L_d phase. The solubility of 16:0-SM (*A*) and 24:0-SM (*B*) in the L_d phase was measured in POPC bilayers containing 0 or 20 mol % cholesterol. Above these concentrations, the SMs formed ordered domains. The values are averages of ≥ 3 experiments $\pm$ SD.
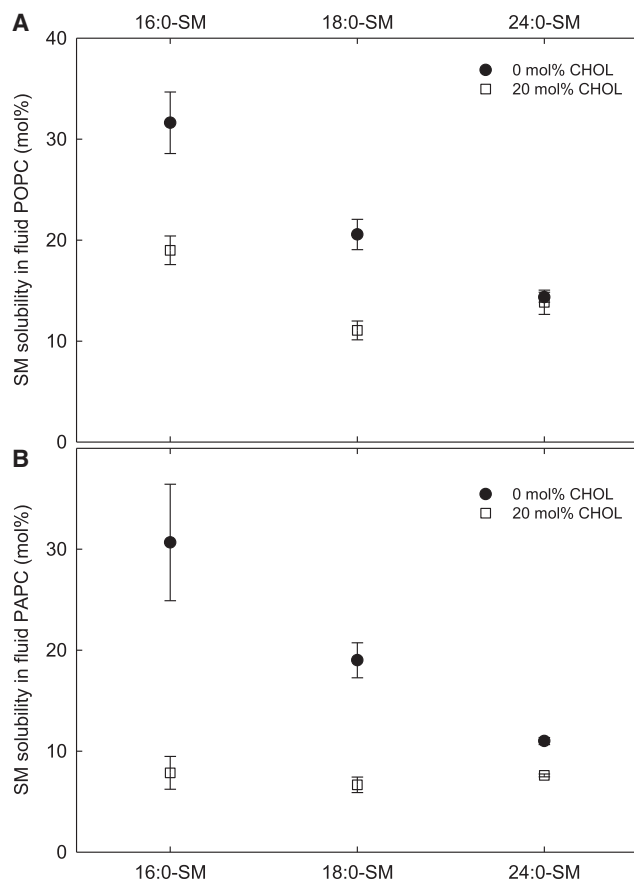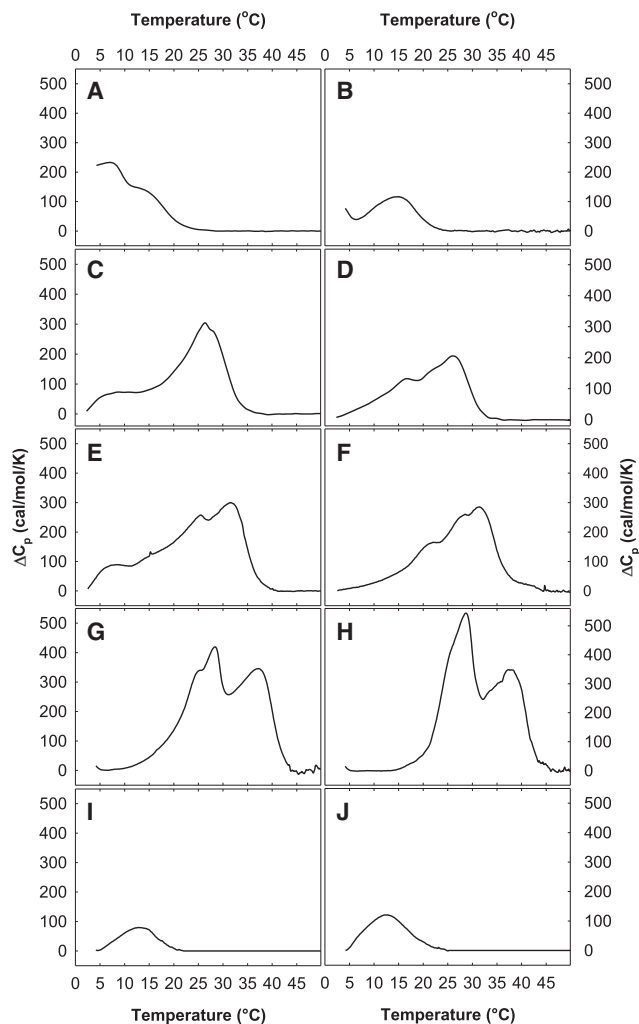

FIGURE 4 Representative thermograms recorded with binary mixtures of SMs and PCs. DSC experiments were performed with binary mixtures (1:1 molar ratio) of different SMs and POPC (*A*, *C*, *E*, *G*, and *I*) or PAPC (*B*, *D*, *F*, *H*, and *J*). The results with 14:0-SM (*A* and *B*), 16:0-SM (*C* and *D*), 18:0-SM (*E* and *F*), 24:0-SM (*G* and *H*), and 24:1-SM (*I* and *J*) are shown. The total amount of lipid was 1.5 mM, and the scan rate was $1°C$ min^{-1}.

range of SMs. The recorded thermograms for these samples are shown in Fig. 4. As is clear from the figure, the thermograms from all lipid combinations were complex and contained several overlapping processes. This was perhaps most clear in 24:0-SM samples that contained two larger peaks. Possibly, this may be due to the large length difference between the acyl chain and the sphingoid base in 24:0-SM. Because of the complexity of the thermograms, we determined the end melting temperatures (i.e., the temperature at which all gel domains in the membranes had melted; Fig. 6).

In both POPC and PAPC bilayers, the overall gel domain stability and end melting temperatures increased with the length of SM acyl chains, except with 24:1-SM. The double bond in 24:1-SM clearly lowered the thermostability of gel domains. We could detect gel domains with 14:0-SM, but the gel to fluid transition occurred at a temperature too low to be measured as a whole, which also motivated the use of the end melting parameter instead of a midtransition parameter. Overall, the thermotropic phase behavior of the SM-PC bilayer was more affected by which SM molecule

was present than whether the PC molecules were PAPC or POPC. This suggested that the gel domains formed by different SM molecules in PAPC and POPC were similar despite the difference in double bonds in the *sn*-1 chains of PC molecules.

Thermostability of SM-enriched domains in ternary bilayers

The thermostability of SM-enriched lateral domains was investigated on the basis of FRET measurements between DPH and Rho-DOPE. As DPH partitions rather equally between disordered and ordered (gel or L_o) domains and Rho-DOPE strongly favors disordered domains, the degree of

lateral segregation can be evaluated from the degree of FRET between the two probes (33). The L_o domains formed by five different SMs in POPC, PAPC, and DOPC bilayers were investigated. DOPC was included in these experiments to allow comparison of sizes of domains formed by hybrid and nonhybrid lipids (34,35). The results are shown in Fig. 5. When the FRET efficiency in the lower end of the temperature range was compared, it became clear that the FRET efficiency is always higher in POPC bilayers than in PAPC or DOPC bilayers. This suggests that the L_o domains formed in POPC bilayers were smaller, as may be expected according to published data (35,36). Using the same parameter, it also seemed that L_o domains were larger in DOPC bilayers than in PAPC bilayers, although the extent depended on the composition of SM acyl chains. According to the FRET data, the largest domains were formed in bilayers with 16:0-SM and the smallest in bilayers with 24:1-SM (Fig. S1). This was the case in POPC, PAPC, and DOPC bilayers.

As the temperature increased, the FRET efficiency increased in all systems. At the higher end of the temperature range, the FRET efficiencies were similar in all studied lipid systems, resulting from homogenous membrane structures without lateral domains. The effect of temperature on FRET efficiency depends on the thermostability of the domains. From the data provided in Fig. 5, it is clear that the compositions of both the PC and SM acyl chains affected the L_o domain stability. We determined the end melting temperature from FRET efficiency curves as the temperature in which the FRET efficiency reached a maximum (shown in Fig. 6). The data show that in POPC, the L_o domains are stabilized by longer SM acyl chains. However, more than 16 carbons in the chains did not significantly increase the thermostability of the domains. In PAPC and DOPC, an increase from 14 to 16 carbons markedly stabilized the domains, whereas a further increase to 18 carbons did not affect domain stability. With 24 carbon-long saturated acyl chains, the thermostability of L_o domains decreased compared to 16 or 18 carbon-long chains.
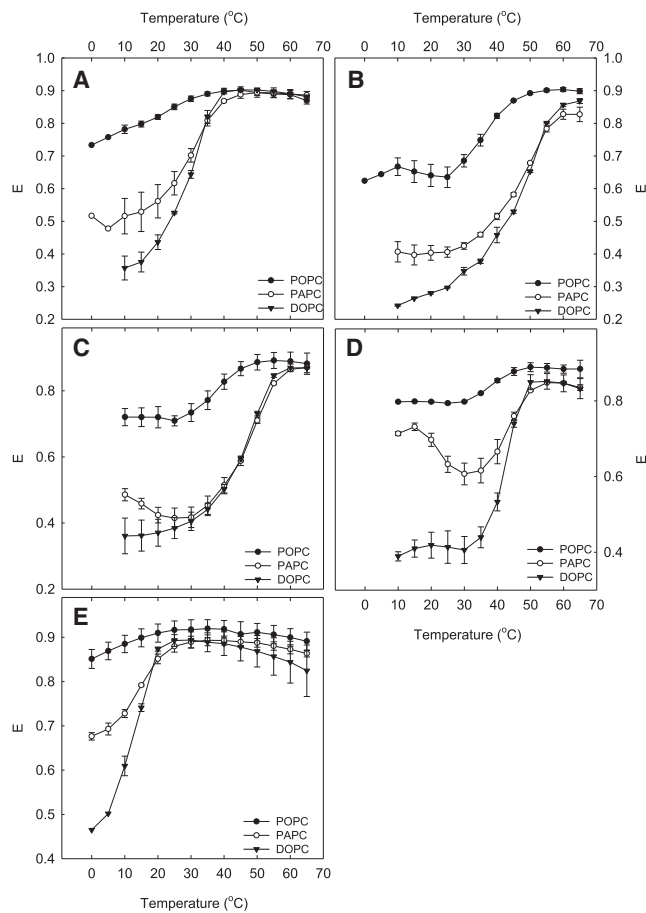
FIGURE 5 The thermostability of the ordered SM-enriched domains as reported by FRET. Samples composed of unsaturated PC:SM:cholesterol (40:40:20) were prepared. Three different PCs were used together with 14:0-SM (*A*), 16:0-SM (*B*), 18:0-SM (*C*), 24:0-SM (*D*), and 24:1-SM (*E*). The F_0 samples contained 0.5 mol % DPH, and the *F* samples contained 0.5 mol % DPH and 2 mol % Rho-DOPE. The fluorescence intensity of the samples was measured with 5°C temperature intervals. The values are averages of $\geq$ 3 experiments $\pm$ SD.
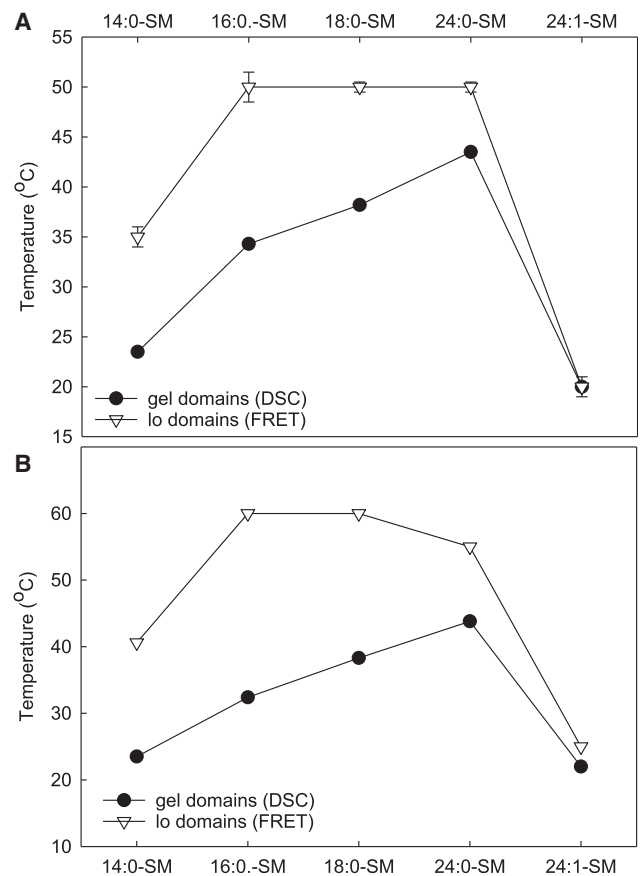
FIGURE 6 A comparison of the thermostability of binary PC:SM systems with 0 and 20 mol % cholesterol. The end melting temperatures determined from the DSC and FRET experiments in (*A*) POPC and (*B*) PAPC bilayers are shown.

It is further of interest to compare the thermotropic behavior of binary PC-SM bilayers, with and without 20 mol % cholesterol. Therefore, we compared the end melting temperatures obtained from DSC and FRET techniques (Fig. 6). The end melting temperature was determined as the temperature in which the DSC and FRET curves stabilized. To validate the use of the end melting parameters, we also calculated the center of mass of endotherms as a measure of the overall gel domain stability for some SM systems and compared them with T_m:s from FRET data (data not shown). As this resulted in similar differences between cholesterol-free and -containing bilayers, we concluded that the end melting parameters were representative of the systems of interest. The difference between the end melting temperatures of gel and L_o domains is shown in Fig. 7. From the data shown in the figure, it is clear that the length of SM acyl chains affected how the presence of cholesterol affected the thermostability of lateral domains. The largest stabilizing effect of cholesterol was observed with 16:0-SM in both POPC and PAPC. In membranes with SMs that had shorter or longer than 16-carbon acyl chains, cholesterol had less impact on thermostability. Overall, the results were similar in POPC and PAPC; however, the stabilizing effect of cholesterol was larger in PAPC bilayers than in POPC with all SMs.

DISCUSSION

When a phospholipid bilayer contains a high enough cholesterol concentration, lateral segregation into L_d and fluid-ordered domains may occur. However, the probability that ordered domains form, as well as the properties of these domains, depend on the structure of phospholipids in the bilayer. In bilayers consisting of only an unsaturated lipid, such as POPC, and cholesterol, lateral segregation is not

expected to occur (2,37). However, some degree of nonrandom mixing may occur (38). Binary mixtures of cholesterol and saturated phospholipids, such as PSM or DPPC, have been reported to have complex thermotropic phase behavior, as shown in published phase diagrams (39–42). However, later studies using FRET and x-ray spectroscopy have failed to detect lateral segregation in such lipid bilayers (2,43). Molecular dynamics simulations of DPPC-cholesterol bilayers have predicted some nanoscale organization into cholesterol-rich and -poor clusters (44), and electron spin resonance data have been interpreted to indicate lateral segregation in PSM-cholesterol bilayers (37,45). One can, therefore, conclude that if there is lateral segregation in bilayers composed of a single saturated phospholipid and cholesterol, domains are likely to be no larger than a few nanometers in diameter and beyond the resolution of most experimental techniques. Hence, it seems that for cholesterol to induce phase separation or even the formation of lateral domains of a larger size, the bilayer should contain at least two phospholipids, in addition to cholesterol. Further, the lateral segregation of membrane components into fluid-ordered and L_d domains or phases requires that the two phospholipids have a tendency to repel each other without cholesterol (16). We have recently reported that the degree to which cholesterol facilitates lateral segregation relates to how favorably it interacts with the phospholipids present in the bilayer (6,9), and others have also presented similar results (18,46). Below, we have discussed the role of cholesterol as a promoter of lateral segregation on the basis of the data presented in this study.

Lateral segregation

We previously observed that cholesterol facilitated lateral segregation in ternary bilayers with PSM as the high-mid-melting temperature (T_m) phospholipid, whereas no or very limited facilitation occurred in similar bilayers with DPPC (47). This may be explained by the markedly lower affinity of cholesterol for DPPC compared to PSM. Next, we wanted to investigate how the structure of SM molecules influenced the interactions with cholesterol and thereby the lateral segregation in the bilayer. As a number of different SMs can be found in mammalian membranes (19), it is important to understand if and how their structural differences could affect their role in the functioning of the membranes.

Using the previously established tPA fluorescence-based method, we determined the solubility limits of different SMs in the L_d phase of POPC and PAPC bilayers (Fig. 1). Above this solubility limit, lateral ordered domains formed, which were detected by analyzing fluorescence lifetime data. With 14:0-SM and 24:1-SM, no formation of gel or L_o domains was observed at 23°C (data not shown). This was in good agreement with published data on 24:1-SM (20). In both POPC and PAPC bilayers, the solubility limit
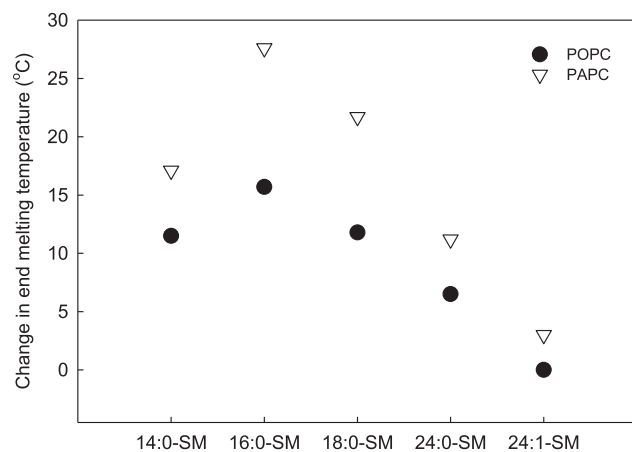

FIGURE 7 The effect of cholesterol on the thermostability of SM-enriched domains. The difference between the end melting temperatures from the DSC (0 mol % cholesterol) and FRET (20 mol % cholesterol) experiments with different SMs in POPC and PAPC bilayers.

of SM without cholesterol clearly increased in the order of 24:0-SM < 18:0-SM < 16:0-SM (Fig. 2). In other words, the longer the SM acyl chains, the lower the solubility in the unsaturated PC. With an increasing chain length, the T_m of SMs increases (48). In fact, the solubility limit of SMs in fluid PC bilayers seems to correlate well with the T_m:s of SM molecules. Accordingly, the miscibility of SMs and PCs is expected on the basis of how the T_m:s of individual lipids are thought to influence the phase behavior of binary mixtures of lipids (49).

In the presence of 20 mol % cholesterol, the solubility limit of SMs in fluid POPC and PAPC bilayers seemed to depend less on the composition of SM acyl chains. This was most evident in PAPC bilayers where SM-enriched L_o domains started to form at ∼7 mol % SM, irrespective of the composition of acyl chains. By comparing how much SM the fluid phase can solubilize before ordered (gel or L_o) domains are formed with and without cholesterol, one gains insights into how much cholesterol promotes lateral segregation in bilayers with a particular lipid composition. From Fig. 2, it is clear that the addition of 20 mol % cholesterol promoted lateral segregation and the formation of L_o domains in all the tested lipid combinations, except in POPC/24:0-SM. In PAPC bilayers, cholesterol promoted lateral segregation more than it did in POPC bilayers, and with the three additional double bonds in the PC sn-2 chain, lateral segregation was even promoted with 24:0-SM. This supports the previously reported results (6), showing that increased amounts of double bonds in the unsaturated PC lead to a stronger promotion of lateral segregation by cholesterol (likely because of less favorable cholesterol-PC interactions). When comparing how cholesterol influenced lateral segregation in combination with different SMs, it is clear from the PAPC results (Fig. 2 B) that the longer the SM acyl chains, the smaller the promoting effect of cholesterol. In POPC, this was less clear, except with 24:0-SM (Fig. 2 A).

Previously, we showed that when the affinity of cholesterol for the high-T_m phospholipid is closer to that for the low-T_m lipid, cholesterol promoted lateral segregation less (6). Accordingly, the less effective promotion of lateral segregation by cholesterol in combination with longer SM acyl chains could be due to less favorable interactions between cholesterol and these SMs. The efflux of cholesterol from monolayers composed of SMs with different acyl chain length has been shown to be rather similar (21). We observed a similar trend in performing similar experiments with the equilibrium partitioning between vesicles composed of different SMs and methyl-β-cyclodextrin (Fig. S2)—that is, the affinity of cholesterol for SM bilayers was rather similar in 16:0-SM, 18:0-SM, and 24:0-SM bilayers. For 24:1-SM bilayers, the affinity was slightly lower, but it was still markedly higher than that for DPPC bilayers. However, when the equilibrium partitioning between methyl-β-cyclodextrin and POPC:X:0-SM (80:20) bilayers was measured, the affinity of cholesterol was found to be highest for bilayers with 16:0-SM and markedly lower for those with 24:0-SM (48). This may be explained by the mismatch between the length of the 24:0 acyl chain in SM and the shorter chains in POPC. Similarly, cholesterol has a lower affinity for 16:0-SM in di-14:1-PC than for 16:-SM in di-18:1-PC, in which the SM acyl chain according to ^{2}H-NMR was disordered (10).

We calculated relative partitioning coefficients (K_R) for cholesterol partitioning between PC and SM bilayers with all different PC-SM combinations (for which partitioning data were available) on the basis of the partition experiments with POPC:SM (80:20) and experiments in which POPC and PAPC were compared (6,48). These were plotted against the change in the solubility limit of SM in the L_d POPC and PAPC phases because of the inclusion of cholesterol (Fig. S3). The resulting plot showed a correlation between K_R and cholesterol promotion of lateral segregation, which is in accordance with previous reports (6,9).

It has been well documented that the thermotropic phase behavior of 16:0-SM and long-chain SMs, such as 24:0-SM, is markedly different (50). Therefore, we wanted to make sure that the effects of cholesterol with different SM molecules did not occur only at the chosen experimental temperature (23°C). In addition, it was of interest to test how cholesterol promotion of lateral segregation was affected by temperature.

The results showed that without cholesterol, the solubility of PSM in fluid POPC was strongly dependent on temperature (Fig. 3 A), which is in agreement with published data on the same lipid system (32,51). With 20 mol % cholesterol in the bilayers, the solubility of SM in the L_d POPC phase was markedly less affected by temperature. The solubility limit was more or less unchanged up to 30°C, but when the temperature was raised further, the solubility gradually increased. Accordingly, the promoting effect of cholesterol on lateral segregation was clearly enlarged as the temperature approached physiological temperature. We speculate that this was due to a clearly decreased affinity of cholesterol for POPC with increasing temperature. It has been shown that the affinity of cholesterol for POPC is ∼30% lower at 37°C than at 23°C (48). In the same temperature range, the affinity of cholesterol for PSM may be expected to be less affected by temperature as the temperature range was clearly below the T_m of PSM. With 24:0-SM, the effect of temperature on lateral segregation was smaller than that observed with 16:0-SM without cholesterol (Fig. 3 B), and the addition of cholesterol did not have any significant effect on temperature dependence at least up to ∼40°C. This indicates that 24:0-SM interacts significantly differently with both cholesterol and POPC compared to 16:0-SM in a wide range of temperatures. We suggest that this is due to less favorable interactions between 24:0-SM and POPC or cholesterol, which is caused by the long acyl chain that gives this SM a relatively high T_m and a clear mismatch in hydrophobic length with the neighboring POPC molecules.

Thermostability of L_o domains

The thermotropic behavior of lipid bilayers composed of more than one lipid offers insights into the interactions between membrane components. Similarly, knowledge about the thermotropic behavior of lateral gel or L_o domains gives us information about the composition of domains as well as a view of the interactions between these components. In this study, we used the DSC technique to study gel domains and the FRET technique to study L_o domains.

In FRET experiments, we used the fluorophore pair DPH (donor) and Rho-DOPE (acceptor). Results obtained with this probe pair have previously been compared to results from deuterium NMR experiments, and the obtained thermostability data were very similar with both methods (10). Next, we compared the thermostability of 15 different lipid systems on the basis of five different SM molecules and three different unsaturated PCs (Fig. 5). The general trend observed with different SMs was that those with unsaturated (24:1-SM) or short acyl chains (14:0-SM) formed less thermostable L_o domains as expected. The thermostability of L_o domains formed by 16:0-SM, 18:0-SM, and 24:0-SM was relatively similar. However, 24:0-SM formed less thermostable L_o domains in PAPC and DOPC than the two shorter SMs, although it had the longest acyl chains.

To evaluate how cholesterol influenced thermostability, the thermostability of L_o domains needs to be compared with the thermostability of the corresponding cholesterol-free systems. The DSC results from such binary PC:SM (1:1) bilayers showed that, first of all, the thermostability of SM-enriched gel domains was clearly dependent on the length of and number of double bonds in the SM acyl chains (Fig. 4). Second, the end melting temperatures of gel domains were very similar in POPC and PAPC bilayers. This suggests that the structure of the high-T_m lipid determined gel domains stability. When we examined the change in end melting temperature upon the addition of 20 mol % cholesterol, it was clear that cholesterol affected the domains of 16:0-SM the most, which are closely followed by 14:0-SM and 18:0-SM, whereas the domains of 24:0-SM and 24:1-SM were only slightly affected by cholesterol (Fig. 7).

The FRET results further provide information about how the sizes of domains were affected by the structure of lipids in the bilayer. However, factors like the domain fractions and probe partitioning also affect the FRET efficiency. It has previously been reported that the structure of acyl chains of unsaturated lipids affects the size of domains formed by cholesterol and saturated phospholipids present in the bilayer (33,52,53). The results in this study are in agreement with these reports, as FRET indicated that the domain size with all SMs was the smallest in POPC bilayers, larger in PAPC bilayers, and the largest in DOPC bilayers (Figs. 5 and S1). However, in the case of DOPC, the decreased FRET efficiency may also be due to an increased fraction

of L_o domains. It seems that the height mismatch between ordered and disordered domains (i.e., line tension), at least in part, controls the size of domains (52–54). However, according to some reported observation, it is possible that other factors are also involved (55,56). For example, it has been proposed that hybrid lipids such as POPC and PAPC can act as linactants and thereby reduce the domain size (34). Our results in this study also agree with this proposition as the largest domains were observed with the nonhybrid lipid DOPC.

When the FRET efficiency before domain melting with different SMs was compared, it became clear that it was the lowest with 16:0-SM in all PC bilayers (Figs. 5 and S1). Although the difference was smaller than that between POPC and DOPC, it seemed that the largest or the most L_o domains were obtained with 16:0-SM, and the SM molecules with both shorter and longer acyl chains formed smaller or less domains (which is in agreement with previously published quenching data (48)). Accordingly, the L_o domains formed by 24:0-SM were significantly smaller and/or less abundant than those formed by 16:0-SM. Because this was the opposite of what was expected when the acyl chain was increased (based on the discussion above), it is possible that the length mismatch between the acyl chain and the sphingoid base in 24:0-SM affects the domain properties. This could be through interdigitation or other molecular rearrangements to optimize lipid packing in the bilayers. Another possible explanation is that the interactions between 24:0-SM and cholesterol are not as favorable as those between 16:0-SM and cholesterol (48). If, for example, the 24 carbon-long chain would be bent in the bilayer center, this could affect how cholesterol interacts with the SM. Further, as it has been shown that cholesterol can lower line tension (57), it is then also possible that cholesterol affected line tension differently with the different SMs.

In summary, the FRET data suggest that cholesterol interacted differently with different SMs and that gave SM-enriched L_o domains that were formed by the different SMs' different properties (size and thermostability). On the basis of the results of this study and previously published data (48), we speculate that this in part was due to a different affinity of cholesterol for different SMs, leading to different SM:cholesterol ratios in the formed L_o domains.

CONCLUSIONS

In this study, we aimed to deepen our understanding of how the structural features of lipids affect the propensity of membranes to undergo lateral segregation. In particular, we focused on the interactions between cholesterol and SMs with different acyl chains. Using previously established experimental approaches, we determined that cholesterol increased lateral segregation tendency the most with

16:0-SM and the least with 24:0-SM. Similarly, cholesterol thermally stabilized SM-enriched domains most with 16:0-SM. As the largest L_o domains also appeared to be formed in membranes with 16:0-SM, it seemed that this SM was especially affected by the presence of cholesterol. This is supported by partitioning studies indicating that cholesterol (in ternary PC:SM:cholesterol bilayers) has the highest affinity for SM with 16 carbon-long saturated chains (48). In binary SM:cholesterol bilayers, however, the affinity of cholesterol is equal for SMs with saturated acyl chains of different lengths (results herein and (21)). Together with previously published results (10), these results indicated that cholesterol-SM interactions are affected by interactions with other phospholipids in the bilayer and how these affect the conformation of the SM. Although this is not very surprising, it is important to take this into consideration when assessing the propensity of a lipid system to form L_o domains. From a biological point of view, our results indicate that structurally different SMs may affect the membrane structure and function differently and that both the content of cholesterol and the structure of the other phospholipids present in the bilayer determined the exact nature of this influence.

SUPPORTING MATERIAL

Supporting Material can be found online at https://doi.org/10.1016/j.bpj.2020.07.014.

AUTHOR CONTRIBUTIONS

T.K.M.N., O.E., and J.P.S. planned the research. O.E., V.H., and K.-L.L. performed the experiments. All authors analyzed the data. T.K.M.N. wrote the article, with contributions from the other authors.

ACKNOWLEDGMENTS

REFERENCES

1. van Meer, G., D. R. Voelker, and G. W. Feigenson. 2008. Membrane lipids: where they are and how they behave. *Nat. Rev. Mol. Cell Biol.* 9:112–124.

2. Feigenson, G. W. 2009. Phase diagrams and lipid domains in multicomponent lipid bilayer mixtures. *Biochim. Biophys. Acta.* 1788:47–52.

3. Veatch, S. L., and S. L. Keller. 2005. Seeing spots: complex phase behavior in simple membranes. *Biochim. Biophys. Acta.* 1746:172–185.

4. Quinn, P. J., and C. Wolf. 2009. The liquid-ordered phase in membranes. *Biochim. Biophys. Acta.* 1788:33–46.

5. Ipsen, J. H., G. Karlström, …, M. J. Zuckermann. 1987. Phase equilibria in the phosphatidylcholine-cholesterol system. *Biochim. Biophys. Acta.* 905:162–172.

6. Engberg, O., V. Hautala, …, T. K. M. Nyholm. 2016. The affinity of cholesterol for different phospholipids affects lateral segregation in bilayers. *Biophys. J.* 111:546–556.

7. Williams, J. A., C. D. Wassall, …, S. R. Wassall. 2013. An electron paramagnetic resonance method for measuring the affinity of a spin-labeled analog of cholesterol for phospholipids. *J. Membr. Biol.* 246:689–696.

8. Niu, S. L., and B. J. Litman. 2002. Determination of membrane cholesterol partition coefficient using a lipid vesicle-cyclodextrin binary system: effect of phospholipid acyl chain unsaturation and headgroup composition. *Biophys. J.* 83:3408–3415.

9. Nyholm, T. K. M., S. Jaikishan, …, J. P. Slotte. 2019. The affinity of sterols for different phospholipid classes and its impact on lateral segregation. *Biophys. J.* 116:296–307.

10. Nyholm, T. K. M., O. Engberg, …, J. P. Slotte. 2019. Impact of acyl chain mismatch on the formation and properties of sphingomyelin-cholesterol domains. *Biophys. J.* 117:1577–1588.

11. Leventis, R., and J. R. Silvius. 2001. Use of cyclodextrins to monitor transbilayer movement and differential lipid affinities of cholesterol. *Biophys. J.* 81:2257–2267.

12. Demel, R. A., J. W. Jansen, …, L. L. van Deenen. 1977. The preferential interaction of cholesterol with different classes of phospholipids. *Biochim. Biophys. Acta.* 465:1–10.

13. Huster, D., K. Arnold, and K. Gawrisch. 1998. Influence of docosahexaenoic acid and cholesterol on lateral lipid organization in phospholipid mixtures. *Biochemistry.* 37:17299–17308.

14. Nyström, J. H., M. Lönnfors, and T. K. M. Nyholm. 2010. Transmembrane peptides influence the affinity of sterols for phospholipid bilayers. *Biophys. J.* 99:526–533.

15. Yeagle, P. L., and J. E. Young. 1986. Factors contributing to the distribution of cholesterol among phospholipid vesicles. *J. Biol. Chem.* 261:8175–8181.

16. Feigenson, G. W. 2006. Phase behavior of lipid mixtures. *Nat. Chem. Biol.* 2:560–563.

17. Wang, C., M. R. Krause, and S. L. Regen. 2015. Push and pull forces in lipid raft formation: the push can be as important as the pull. *J. Am. Chem. Soc.* 137:664–666.

18. Wang, C., Y. Yu, and S. L. Regen. 2017. Lipid raft formation: key role of polyunsaturated phospholipids. *Angew. Chem. Int.Engl.* 56:1639–1642.

19. Peter Slotte, J. 2013. Molecular properties of various structurally defined sphingomyelins – correlation of structure with function. *Prog. Lipid Res.* 52:206–219.

20. Maté, S., J. V. Busto, …, F. M. Goñi. 2014. N-nervonoylsphingomyelin (C24:1) prevents lateral heterogeneity in cholesterol-containing membranes. *Biophys. J.* 106:2606–2616.

21. Ramstedt, B., and J. P. Slotte. 1999. Interaction of cholesterol with sphingomyelins and acyl-chain-matched phosphatidylcholines: a comparative study of the effect of the chain length. *Biophys. J.* 76:908–915.

22. Fischer, R. T., F. A. Stephenson, …, F. Schroeder. 1984. Delta 5,7,9(11)-Cholestatrien-3 beta-ol: a fluorescent cholesterol analogue. *Chem. Phys. Lipids.* 36:1–14.

23. Ohvo-Rekilä, H., B. Akerlund, and J. P. Slotte. 2000. Cyclodextrin-catalyzed extraction of fluorescent sterols from monolayer membranes and small unilamellar vesicles. *Chem. Phys. Lipids.* 105:167–178.

24. Kuklev, D. V., and W. L. Smith. 2004. Synthesis of four isomers of parinaric acid. *Chem. Phys. Lipids.* 131:215–222.

25. Sklar, L. A., B. S. Hudson, and R. D. Simoni. 1977. Conjugated polyene fatty acids as fluorescent probes: synthetic phospholipid membrane studies. *Biochemistry.* 16:819–828.

26. Rouser, G., S. Fkeischer, and A. Yamamoto. 1970. Two dimensional then layer chromatographic separation of polar lipids and determination of phospholipids by phosphorus analysis of spots. *Lipids.* 5:494–496.

27. Jungner, M., H. Ohvo, and J. P. Slotte. 1997. Interfacial regulation of bacterial sphingomyelinase activity. *Biochim. Biophys. Acta.* 1344:230–240.

28. Sklar, L. A., and B. S. Hudson. 1976. Conjugated polyene fatty acids as fluorescent membrane probes: model system studies. *J. Supramol. Struct.* 4:449–465.

29. Sklar, L. A., B. S. Hudson, and R. D. Simoni. 1975. Conjugated polyene fatty acids as membrane probes: preliminary characterization. *Proc. Natl. Acad. Sci. USA.* 72:1649–1653.

30. Nyholm, T. K., D. Lindroos, …, J. P. Slotte. 2011. Construction of a DOPC/PSM/cholesterol phase diagram based on the fluorescence properties of trans-parinaric acid. *Langmuir.* 27:8339–8350.

31. Castro, B. M., R. F. de Almeida, …, M. Prieto. 2007. Formation of ceramide/sphingomyelin gel domains in the presence of an unsaturated phospholipid: a quantitative multiprobe approach. *Biophys. J.* 93:1639–1650.

32. Halling, K. K., B. Ramstedt, …, T. K. Nyholm. 2008. Cholesterol interactions with fluid-phase phospholipids: effect on the lateral organization of the bilayer. *Biophys. J.* 95:3861–3871.

33. Pathak, P., and E. London. 2015. The effect of membrane lipid composition on the formation of lipid ultrananodomains. *Biophys. J.* 109:1630–1638.

34. Hassan-Zadeh, E., E. Baykal-Caglar, …, J. Huang. 2014. Complex roles of hybrid lipids in the composition, order, and size of lipid membrane domains. *Langmuir.* 30:1361–1369.

35. Heberle, F. A., M. Doktorova, …, G. W. Feigenson. 2013. Hybrid and nonhybrid lipids exert common effects on membrane raft size and morphology. *J. Am. Chem. Soc.* 135:14932–14935.

36. Petruzielo, R. S., F. A. Heberle, …, G. W. Feigenson. 2013. Phase behavior and domain size in sphingomyelin-containing lipid bilayers. *Biochim. Biophys. Acta.* 1828:1302–1313.

37. Ionova, I. V., V. A. Livshits, and D. Marsh. 2012. Phase diagram of ternary cholesterol/palmitoylsphingomyelin/palmitoyloleoyl-phosphatidylcholine mixtures: spin-label EPR study of lipid-raft formation. *Biophys. J.* 102:1856–1865.

38. Heerklotz, H., and A. Tsamaloukas. 2006. Gradual change or phase transition: characterizing fluid lipid-cholesterol membranes on the basis of thermal volume changes. *Biophys. J.* 91:600–607.

39. Vist, M. R., and J. H. Davis. 1990. Phase equilibria of cholesterol/dipalmitoylphosphatidylcholine mixtures: 2H nuclear magnetic resonance and differential scanning calorimetry. *Biochemistry.* 29:451–464.

40. Sankaram, M. B., and T. E. Thompson. 1990. Interaction of cholesterol with various glycerophospholipids and sphingomyelin. *Biochemistry.* 29:10670–10675.

41. Huang, T. H., C. W. Lee, …, R. G. Griffin. 1993. A 13C and 2H nuclear magnetic resonance study of phosphatidylcholine/cholesterol interactions: characterization of liquid-gel phases. *Biochemistry.* 32:13277–13287.

42. McMullen, T. P., and R. N. McElhaney. 1995. New aspects of the interaction of cholesterol with dipalmitoylphosphatidylcholine bilayers as revealed by high-sensitivity differential scanning calorimetry. *Biochim. Biophys. Acta.* 1234:90–98.

43. Mills, T. T., G. E. Toombes, …, J. F. Nagle. 2008. Order parameters and areas in fluid-phase oriented lipid membranes using wide angle X-ray scattering. *Biophys. J.* 95:669–681.

44. Javanainen, M., H. Martinez-Seara, and I. Vattulainen. 2017. Nanoscale membrane domain formation driven by cholesterol. *Sci. Rep.* 7:1143.

45. Collado, M. I., F. M. Goñi, …, D. Marsh. 2005. Domain formation in sphingomyelin/cholesterol mixed membranes studied by spin-label electron spin resonance spectroscopy. *Biochemistry.* 44:4911–4918.

46. Wang, C., P. F. Almeida, and S. L. Regen. 2018. Net interactions that push cholesterol away from unsaturated phospholipids are driven by enthalpy. *Biochemistry.* 57:6637–6643.

47. Engberg, O., T. Yasuda, …, J. P. Slotte. 2016. Lipid interactions and organization in complex bilayer membranes. *Biophys. J.* 110:1563–1573.

48. Jaikishan, S., and J. P. Slotte. 2011. Effect of hydrophobic mismatch and interdigitation on sterol/sphingomyelin interaction in ternary bilayer membranes. *Biochim. Biophys. Acta.* 1808:1940–1945.

49. Mabrey, S., and J. M. Sturtevant. 1976. Investigation of phase transitions of lipids and lipid mixtures by sensitivity differential scanning calorimetry. *Proc. Natl. Acad. Sci. USA.* 73:3862–3866.

50. Björkqvist, Y. J., J. Brewer, …, B. Westerlund. 2009. Thermotropic behavior and lateral distribution of very long chain sphingolipids. *Biochim. Biophys. Acta.* 1788:1310–1320.

51. de Almeida, R. F., A. Fedorov, and M. Prieto. 2003. Sphingomyelin/phosphatidylcholine/cholesterol phase diagram: boundaries and composition of lipid rafts. *Biophys. J.* 85:2406–2416.

52. Heberle, F. A., R. S. Petruzielo, …, J. Katsaras. 2013. Bilayer thickness mismatch controls domain size in model membranes. *J. Am. Chem. Soc.* 135:6853–6859.

53. García-Sáez, A. J., S. Chiantia, and P. Schwille. 2007. Effect of line tension on the lateral organization of lipid membranes. *J. Biol. Chem.* 282:33537–33544.

54. Usery, R. D., T. A. Enoki, …, G. W. Feigenson. 2017. Line tension controls liquid-disordered + liquid-ordered domain size transition in lipid bilayers. *Biophys. J.* 112:1431–1443.

55. Bleecker, J. V., P. A. Cox, and S. L. Keller. 2016. Mixing temperatures of bilayers not simply related to thickness differences between L_o and L_d phases. *Biophys. J.* 110:2305–2308.

56. Bleecker, J. V., P. A. Cox, …, S. L. Keller. 2016. Thickness mismatch of coexisting liquid phases in noncanonical lipid bilayers. *J. Phys. Chem. B.* 120:2761–2770.

57. Tsai, W. C., and G. W. Feigenson. 2019. Lowering line tension with high cholesterol content induces a transition from macroscopic to nanoscopic phase domains in model biomembranes. *Biochim. Biophys. Acta Biomembr.* 1861:478–485.